Volume 4, Issue 8, August 2014 ISSN: 2277 128X

International Journal of Advanced Research in Computer Science and Software Engineering

Research Paper

Available online at: www.ijarcsse.com

Functional Discrimination of fMRI Data from Multiple Subjects

Ngoc Dung Bui* Management & Science University Malaysia

David Arsivatham University of Malaya Malaysia

Md Gapar Md Dota Management & Science University Malaysia

Abstract— In this paper, we proposes a new model-free approach to analyse fMRI time series data. Instead of testing a parametric model which estimates a brain regional activity during a cognitive task, we use the synchronization of fMRI voxels as the basis of our analysis. Synchronization between large voxel cross sections are expected when the brain responds to a stimulus. The paper shows using a simple definition of synchronization that the phenomenon is insensitive to the choice of thresholds over a broad range of thresholds, and is thus statistically more robust than the average activation profile, which depends sensitively on the baseline assumed. We then explains how a functional picture of the brain's response to a visual-motor task can be obtained by examining differential fractional synchronizations in the primary motor cortex, the supplementary motor cortex, the primary visual cortex, and the occipital cortex. Finally, the paper demonstrates an unbiased method to compare multiple subjects functionally by constructing and singular value decomposing a discrimination matrix enumerating the different synchronization patterns seen in the different subjects.

Keywords— fMRI time series; synchronization; functional discrimination; subject-to-subject comparisons; singular value decomposition

I. INTRODUCTION

Functional Magnetic Resonance imaging (fMRI) is an imaging technology which is primary used to perform brain activation studies by measuring the Blood Oxygen Level Dependent (BOLD) signal [1]. During the course of an fMRI experiment, a series of brain images are acquired with each image consisting of thousands of voxels while the subject performs a set of tasks. Changes in the measured signal between individual images are then used to make inferences regarding task-related activations in the brain. fMRI experiments can be performed to retrieve brain responses to different tasks in a single subject, as well as to the same task in different subjects , and the comparison of these responses have allowed us to better understand how the brain works [2]. In particular, there is great potential for using fMRI to characterize brain disorders such as Alzheimer's disease [3, 4], Parkinson's disease [5], and schizophrenia [6].

In a typical fMRI data set, it is common to determine which voxels are activated by the stimulation. The common practice is to first to perform statistical parametric model (SPM) analysis of each voxel independently. The estimated parameters from this analysis are compared with the data and can be used to create images of brain activation, but more importantly, they can go into statistics tests to be assessed for significance [7]. However, the approach does not take into account the spatial nature of the image data by examining voxels in isolation. Moreover, the time series of individual voxels frequently appear very noisy, making it hard to reliably identify the responses to tasks. These problems are partially solved by averaging the fMRI time series over large brain areas [8]. However, the selection of brain area is subjective, and there exists many anatomical maps of the brain [9, 10]. Through statistically clustering voxels whose activation patterns are most similar before averaging over them, this selection problem can be solved [11, 12]. Nevertheless, simple averaging has not been able to make full use of the information contained in all voxels.

When multiple subjects are employed, it is common for studies to average data across subjects given the same task [13]. For an inhomogeneous group of subjects, this method gives the wrong picture of subject-subject variation. Most fMRI studies that do not concentrate on diagnostic classification make use of simple group averaging to differentiate between subject classes such as age or clinical conditions. Naturally, the group average need not be representative of the diverse fMRI activation behaviours across subjects within the same group. Consequently, the group-averaged activation profiles cannot be used for the more demanding problem of classification, because there is simply no prediction accuracy so to speak. As fMRI data sets become larger, this classification problem becomes more severe, because some manually curated classifiers may be statistically meaningful, while other classifier might not. In general, these meaningful classifiers are not known beforehand. There is thus an urgent need for the development of automated classification algorithms that can mine the ever-growing databases of fMRI data for truly usable knowledge discovery.

In this paper we present in Section 2 a model-free approach to analyze fMRI data. Instead of SPM analysis based on the general linear model (GLM) to identify voxels that are significantly activated [14], we observe that for a brain area to be strongly activated, the voxel in this area must be synchronized. If we look at synchronization instead of activation, we do not need to assume any model for the time series data and the baseline accurately. The synchronization patterns of

different parts of the brain then give us a functional picture of how it responds to stimuli. This allows us to do a direct functional comparison between multiple subjects sharing a common task sequence or an indirect functional comparison through a discrimination matrix if each subject is given a different task sequence. In Section 3, we show the results of our synchronization analysis of an fMRI data set collected from a group of 13 Alzheimer's disease and 14 normal subjects. In this section, we discuss the implications of our approach in understanding brain dynamic and for diagnostics before concluding in Section 4.

II. METHODOLOGY

In general, we start analyzing fMRI data by grouping voxels into those whose signals we are interested in and those whose signals we are not interested in [15]. Signals that we deemed uninteresting may be physiology-related or motion-related. Normally, the task presented to the subject triggers a signal that rises distinctively above the noise level. Such signals can therefore be used to distinguish actual brain activation and noise. More importantly, we never find isolated voxels responding to a task. Activated voxels are almost always grouped into active regions in the brain. For a particular active region, many voxels must be activated at the same or similar times in order for the response to be strong. This implies that a large cross section of voxels must be synchronized in response to a stimulus. These cross sections of voxels can be discovered through statistical clustering based on the magnitude of their responses to the experiment [11].

In the literature, we find different ways to measure synchronization, such as coherence [16] and the duration of coupling between a pair of (neurophysiological) processes [17]. Coherence measures synchronization in the frequency domain, by comparing the average cross and power spectra of the two time series across the low-frequency band. As such, it is given by

$$Coh = \frac{2}{K(K-1)} \sum_{x=1}^{K-1} \sum_{y=x+1}^{K} \bar{C}oh_{xy}(\lambda) \tag{1}$$

where K is the number of voxels within the ROI, and λ is a frequency in the low-frequency band. Here,

$$\bar{C}oh_{xy}(\lambda) = \frac{\left| \sum_{\lambda} \hat{f}_{xy}(\lambda) \right|^2}{\sum_{\lambda} \hat{f}_x(\lambda) \sum_{\lambda} \hat{f}_y(\lambda)} \tag{2}$$

is the band-averaged coherence of two time series, and

$$\hat{f}_{xy}^{(T)}(\lambda) = \frac{1}{N} \sum_{n=1}^{N} X_n^{(T)}(\lambda) Y_n^{*(T)}(\lambda) \tag{3}$$

is the cross spectrum of two time series $x(t)$ and $y(t)$, with $X_n^{(T)}(\lambda)$ and $Y_n^{(T)}(\lambda)$ is the discrete Fourier transforms of the n^{th} segment of time series $x(t)$ and $y(t)$ respectively. Similarly,

$$\hat{f}_x^{(T)}(\lambda) = \frac{1}{N} \sum_{n=1}^{N} \left| X_n^{(T)}(\lambda) \right|^2, \tag{4}$$

$$\hat{f}_y^{(T)}(\lambda) = \frac{1}{N} \sum_{n=1}^{N} \left| Y_n^{(T)}(\lambda) \right|^2 \tag{5}$$

are the power spectra of time series $x(t)$ and $y(t)$ respectively.

The duration of coupling between a pair of neurophysiological processes is the length of time that their bandpass-filtered signals are in phase synchronization with each other. A pair of time series $F_i(t)$ and $F_j(t)$ is phase synchronized if their phase difference

$$\Delta\phi_{ij}(t) = Arg(\bar{C}_{ij}(t)) \tag{6}$$

is smaller than some arbitrary value. Here

$$\bar{C}_{ij}(t) = \frac{\left\langle W_k^*(F_i) W_k(F_j) \right\rangle}{\sqrt{\left\langle \left| W_k(F_i) \right|^2 \right\rangle \left\langle \left| W_k(F_j) \right|^2 \right\rangle}} \tag{7}$$

is the short-time average of the instantaneous complex phase, with W_k being the k^{th} scale of a Hilbert wavelet transform.

In this paper, we chose a simpler definition of synchronization: two voxels are synchronized if their standardized fMRI activities both exceed a given threshold. We will show in Section 3 that this measure of synchronization is robust because it does not depend on the threshold selected.

In Fig. 1 we show the average standardized fMRI signal of the primary motor cortex (Brodmann area 4 (BA4)). Also shown in this figure is the dynamic standard deviation

$$\sigma(t) = \frac{1}{N}\sum_{i=1}^{N}(\zeta_i(t) - \mu(t))^2 \qquad (8)$$

where $\zeta_i(t)$ is the standardized fMRI activity of voxel *i*, and $\mu(t)$ is standardized fMRI activity averaged across all voxels in the given ROI. The dynamic standard deviation gives us a sense of how variable the BOLD signals across voxels are at any given point in time. As we can see, the dynamic standard deviation is mostly constant except during episodes of activation strongly above or below average. In the same figure we show the standardized fMRI signals of two voxels in the primary motor cortex. We observe that the activities of two voxels tend to rise and dip together when the activities are strong, and less so when the activities are weak. Therefore, we believe that the strong activities represent signal, whereas the weak activities represent noise. To differentiate signal from noise, we consider two voxels synchronized only if they emerge together from a rejection band. For the purpose of this paper, we set the rejection band to be $(-\sigma, +\sigma)$, where

$$\sigma = \frac{1}{T}\sum_{t=1}^{T}\sigma(t) \qquad (9)$$

is the time average of the dynamic standard deviation. We then define the positive and negative synchronization fractions at time *t*

$$\rho_+(t) = \frac{1}{N}\sum_{i=1}^{N}\theta(\zeta_i(t) - \sigma), \qquad (10)$$

$$\rho_-(t) = \frac{1}{N}\sum_{i=1}^{N}\theta(-\zeta_i(t) - \sigma) \qquad (11)$$

to be the fractions of voxels whose standardized fMRI signals rise above or fall below $+\sigma(-\sigma)$. Here,

$$\theta(x) = \begin{cases} 1, & x>0; \\ 0, & \text{otherwise} \end{cases} \qquad (12)$$

is the unit step function.

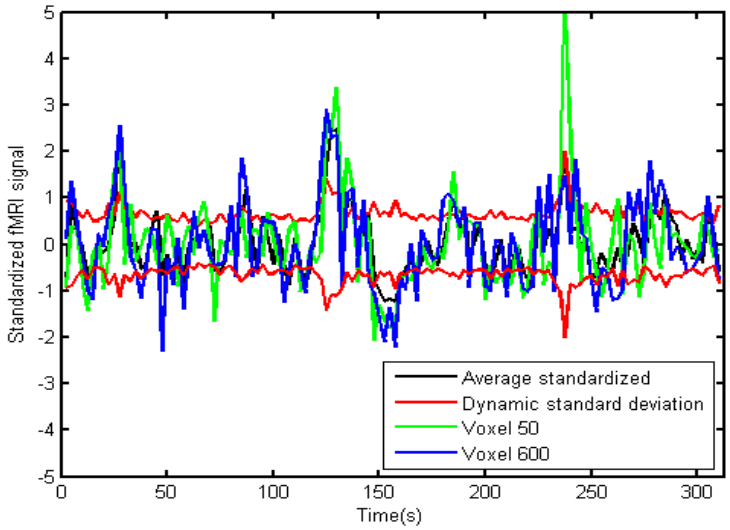

Fig. 1. Average standardized fMRI signal (black) and dynamic standard deviation (red) of the motor cortex in Alzheimer subject 2. Also shown on the plot are the standardized fMRI signals of voxel 50 (green) and voxel 600 (blue). Standardized fMRI activity that goes above the average standard deviation σ can be considered stronger-than-average activation, whereas fMRI activity that goes below $-\sigma$ can be considered weaker-than-average activation.

In Fig. 2 we plot the positive and negative synchronization fractions on top of the average standardized fMRI signal. The positive synchronization peaks coincide with the peaks of average standardized fMRI signal and the negative synchronization peaks coincide with the troughs of the average standardized fMRI signal. The relative strengths of the synchronization peaks are also similar to the relative strengths of the average standardized fMRI peaks. This gives us assurance that the synchronization patterns observed are functionally meaningful.

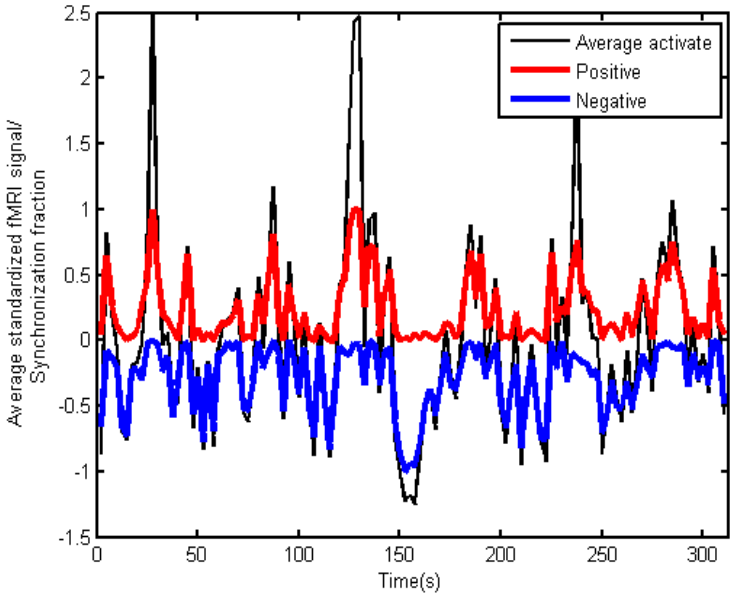

Fig. 2. The synchronization patterns of BA4 in Alzheimer subject 2. In this figure, the black curve is the average standardized fMRI activity, the red curve is the positive synchronization fraction (voxels with standardized fMRI activity exceeding $+\sigma$), and the blue curve is the negative synchronization fraction (voxels with standardized fMRI activity below $-\sigma$).

But what do all these synchronization patterns mean? Let us start by giving an analogy from microelectronics. In a microprocessor we find many transistors. If these transistors can only turn on or turn off altogether, then the microprocessor has no information processing capability. For the microprocessor to process information we must have some transistors in the on state and other transistors in the off state at one given time and a different pattern of transistors that are on and off at a later time. We believe this differentiated response to information must also happen in the brain. Therefore we look out for such differentiated responses in different ROIs in the brain. There are two ways for the responses of different ROIs to be different. First we can have one ROI synchronize before and another ROI does so. Second we can have one ROI synchronize more strongly than another ROI. In fMRI experiments, it may be difficult to see the first type of differentiation because of the low time resolution, so we concentrate on looking for the second type of differentiated response, as shown in Fig. 3.

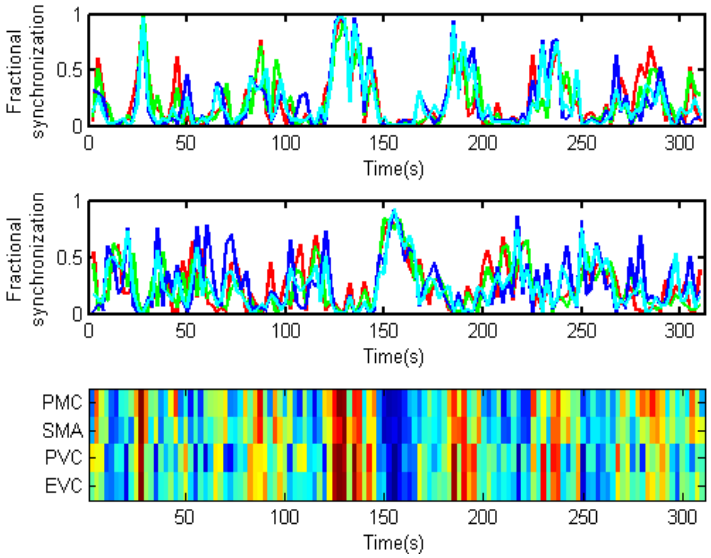

Fig. 3. Positive (top) and negative (middle) synchronization patterns of four Brodmann areas (primary motor cortex (PMC), supplementary motor area (SMA), primary visual cortex (PVC), and extrastriate visual cortical areas (EVC)) in Alzheimer subject 2. These synchronization patterns in the four ROIs can be better visualized in a single color map, where blue indicates strong negative synchronization and red indicates strong positive synchronization. In this color map, green indicates the absence of strong positive or negative synchronizations.

In Fig. 4, we show the synchronization fractions of all ROIs in 13 Alzheimer subjects. If the subjects were given the same task sequence, we would be able to directly compare functional differences in their responses to the tasks. In this figure, the tasks sequence varies from subject to subject. Therefore, though the synchronization patterns are interesting, we cannot directly compare the functional responses of different subjects. For such fMRI data, we must perform functional comparison between different subjects indirectly. We do this by constructing a discrimination matrix.

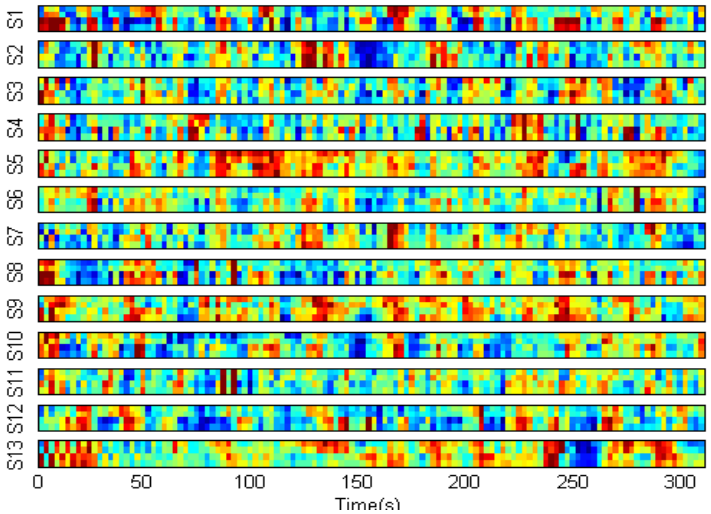

Fig. 4. Synchronization color maps of all ROIs in all 13 Alzheimer subjects.

First we go through the synchronization pattern of an individual subject and ask whether we find an instance of a particular ordering of synchronization fractions. For example, we may find the strongest synchronization in the primary motor cortex (PMC, BA4), the next strongest synchronization in the supplementary motor area (SMA, BA6), followed by the primary visual cortex (PVC, BA17), and then the *extrastriate visual cortical areas* (EVC, BA18 and BA19) for a particular stimulation episode. This is a functional pattern we may find in other subjects as well. We thus exhaust all functional patterns and list the subjects we find these patterns in the form of a non-square matrix. In this discrimination matrix D the rows represent different subjects while the columns represent different functional patterns, such that $D_{ij}=1$ if functional pattern j is found in subject i, and $D_{ij}=0$ otherwise. We then singular value decompose $D=U\Sigma V^T$, where the columns of U are eigenvectors of subjects and the columns of V are eigenvectors of functional patterns.

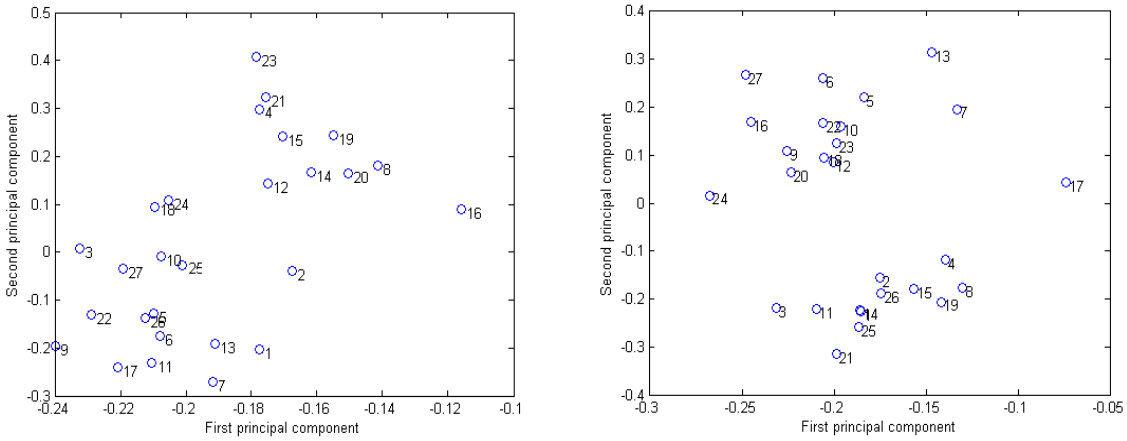

Fig. 5**.** Plots of weights of individual subjects (13 Alzheimer, 14 normal) of the first and second principal components of the discrimination matrices obtained from positive synchronization (left) and negative synchronization (right).

If we are interested in the functional classification of subjects, we can plot the weights of each subject along the first and second principal components of U. Clusters that appear in such a plot give a natural classification scheme (see Fig. 5). Alternatively if we are interested in a natural classification scheme for the functional patterns we can plot the weights of each functional pattern along the first and second principal components of V. Again clusters that might appear in such a plot would allow us to naturally classify functional patterns. Finally, we can combine these two pieces of information in the form of a reordered version of the discrimination matrix, as shown in Fig. 6. To reorder the discrimination matrix, we make use of the fact that the second principal component is generally associated with the greatest difference between subjects. In this second principal component, a subject with positive weight has similar functional patterns compared to another subject with positive weight, but dissimilar functional patterns from a subject with negative weight. We can therefore reorder the subjects, so that those with positive weights come first, followed by those with negative weights. This gives us the reordered discrimination matrix shown in Fig. 6.

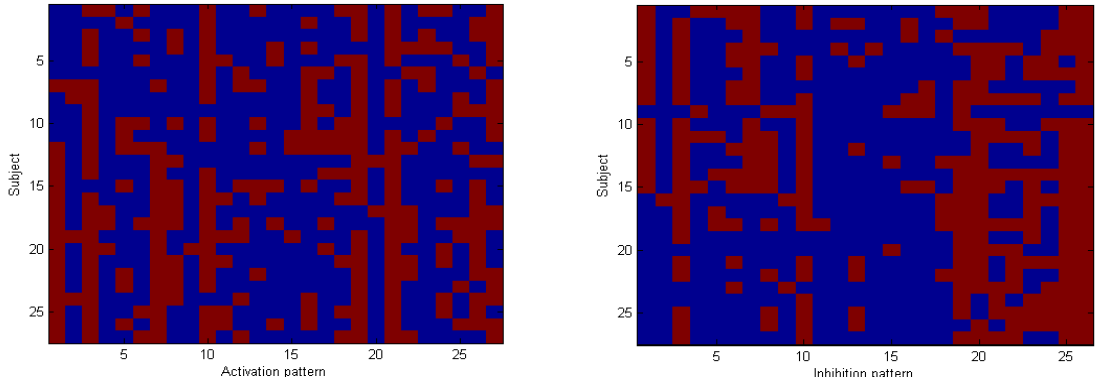

Fig. 6. The reordered discrimination matrices obtained from positive synchronization (left) and negative synchronization (right).

III. EXPERIMENTAL RESULTS

A. Data and Experiments

The data used in this paper is from Washington University [3]: 13 subjects with very mild to AD conditions and 14 normal subjects were scanned in a simple sensory-motor experiment. During the task, subjects are required to respond with a button press with their right index fingers to a stimulus onset. The visual stimulus was a flashing checkerboard that was shown for 1.5 s by itself, or in pairs with a 5.36 s gap between presentations. The raw data were received from the fMRI Data Center at Dartmouth College and preprocessed using SPM5 [18]. Images were motion corrected and normalized to coordinates of Talairach and Tournoux [9]. They were also smoothed with a 4-mm Gaussian kernel to decrease spatial noise.

B. Single Subject

As mentioned earlier, when a brain area becomes activated, not only will there be a statistically significant increase in blood flow that follows, but there will also increase synchronization between different points in the brain area. This can be seen in Fig. 3 (top and middle), where activations peaks are follow by inhibition peaks in all ROIs. To be sure that the synchronization we see is functionally meaningful, we need to check how sensitive it is to the choice of threshold. In Fig. 7, we show the fractional synchronizations for three different thresholds. The positions of the peaks do not change, and the relative strengths of peaks also do not change much. More importantly, the absolute strengths of most peaks remain the same for thresholds up to approximately σ. For higher thresholds, the absolute strengths of most peaks drop dramatically. This tells us that there is a natural cut-off to the threshold we can use to measure synchronization. Below the cutoff the fractional synchronizations measured are highly robust.

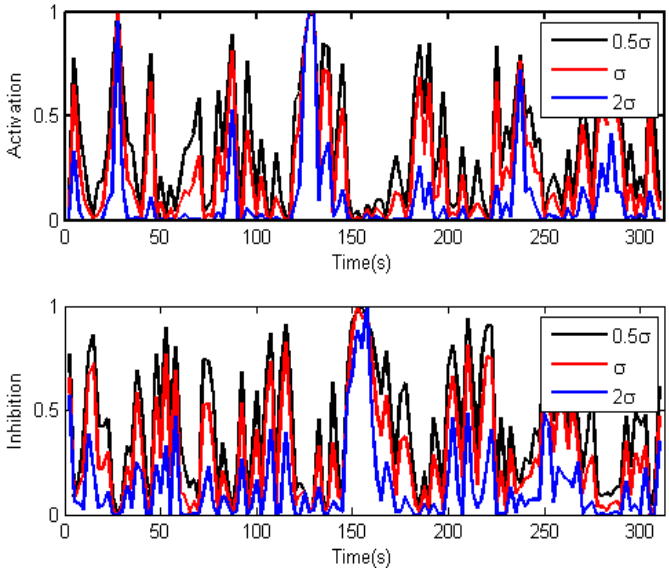

Fig. 7. The positive (top) and negative (bottom) synchronization fractions obtained for BA4 in Alzheimer subject 2 with three different thresholds.

Referring again to Fig. 3, we see that all 4 ROIs are positive synchronized for certain stimulation episodes. In other episodes we can have the motor ROIs becoming synchronized when the visual ROIs are not, and vice versa. In the bottom of Fig. 3, blue indicates negative synchronization while red indicates positive synchronization. If an ROI is green in the color map at a given time point, then there is no significant positive or negative synchronizations. As we can see, at about t = 25, 130, 180 and 230 s, there are strong positive synchronization in all ROIs, whereas at about t = 150 s, there is strong negative synchronization in all ROIs. At about t = 10, 70, 100, 220 s, there are negative synchronizations of motor

areas followed by visual areas, whereas at t = 180 and 280 s, there are positive synchronizations of the motor areas followed by visual areas. Finally, at about t = 80 and 240 s, there are positive synchronizations of visual areas followed by motor areas. Therefore, we see both differentiated and undifferentiated responses in the subjects. For the differentiated responses, we find sometimes motor areas leading visual areas, and sometimes the other way round.

C. Multiple Subjects

In fMRI study of multiple subjects for classification purposes, we would like to find features in the fMRI time series that is present in one group of subjects but not others. If we can do this for every group, then we can identify all groups based on their unique features. Unfortunately, this is generally very difficult. We frequently end up not able to discriminate the multiple groups, or discover clusters containing members from many groups. The holy grail of such classification studies would be to start with no assumptions on which groups an individual belongs to, and discovers his or her grouping automatically. Ideally, we want such groups to be functionally distinct from each other.

The greatest challenge neuroscientists face in this regard is that the variability across subjects may be related to physiological fluctuation, motion or resting-state activity [19]. Because the inter-subject variance is large in comparison with the task-induced difference in BOLD activity, voxel-based analyses that measure the significance of an effect by comparing its mean value to its variability across subjects are typically insensitive [20]. In order to make these statistical tests more sensitive, it is frequently necessarily to assume some consistency in the spatial pattern of subjects across subjects. In the approach described in this paper, we make no assumptions about which functional patterns should be more useful, and which functional patterns would be less useful. Instead, we want to discover all this starting from the data itself.

Referring to Fig. 4, we find that there is no easy way to directly compare the synchronization patterns of different subjects. This is because the sequences of tasks given to the subjects are different. We therefore construct a discrimination matrix to look for hidden functional differences between subjects. From Fig. 5, we find that there are two natural positive synchronization clusters as well as two natural negative synchronization clusters. The compositions of the clusters are shown in Table 1, and we find that the Alzheimer and normal subjects are not differentiated, during positive or negative synchronizations.

Table 1. Compositions of the clusters discovered from the singular value decomposition of the discrimination matrices obtained from the positive and negative synchronizations. The Alzheimer subjects are from 1 to 13, whereas the normal subjects are from 14 to 27.

Synchronization	Cluster 1		Cluster 2	
	Alzheimer	Normal	Alzheimer	Normal
Positive	1, 2, 3, 5, 6, 7, 10, 11, 13	17, 18, 22, 24, 25, 26, 27	4, 8, 12	14, 15, 16, 19, 20, 21, 23
Negative	1, 2, 3, 4, 8, 11	14, 15, 17, 19, 21, 25, 26	5, 6, 7, 9, 10, 12, 13	16, 18, 20, 22, 23, 24, 27

Finally, from the reordered discrimination matrix in Fig. 6 we find mostly non-discriminatory patterns that appear in all subjects. However, we do find discriminatory patterns. In Fig. 6(left), we see that the two clusters of subjects are primarily discriminated by the positive synchronization patterns 1 (PMC>SMA>PVC>EVC), 7 (PMC>EVC>PVC>SMA), 8 (SMA>PMC>PVC>EVC), 16 (PVC>PMC>EVC>SMA), 18 (PVC>SMA>EVC>PMC), 26 (EVC>PVC>PMC>SMA), 27 (EVC>PVC>SMA>PMC), i.e. mostly stronger positive synchronizations in the motor ROIs. In Fig. 6(right) we see that the two clusters of subjects are primarily discriminated by the negative synchronization patterns 1 (PMC>SMA>PVC>EVC), 4 (PMC>PVC>SMA>EVC), 6 (PMC>EVC>SMA>PVC), 7 (PMC>EVC>PVC>SMA), 8 (SMA>PMC>PVC>EVC), 18 (PVC>SMA>EVC>PMC), 19 (PVC>EVC>PMC>SMA), 23 (EVC>SMA>PMC>PVC), 24 (EVC>SMA>PVC>PMC). Here we find the primary motor cortex (BA4) being most frequently the most negatively synchronized, followed by the primary visual cortex (BA17) and the extrastriate visual cortical area (BA18/BA19).

IV. CONCLUSIONS

To conclude, we have presented a model-free approach to analyzing fMRI data to find the meaningful functional difference between subjects. Instead of looking for tell-tale average activation profiles, we examine synchronization patterns in different parts of the brain. Based on these patterns we constructed a discrimination matrix between subjects and between synchronization patterns, whose matrix elements tell us whether a given pair of subjects can be discriminated by a given positive or negative synchronization pattern. When subjects can be classified into natural clusters, we showed that it is possible to identify the most important functional differences between these clusters of subjects. While the approach has been illustrated using fMRI data in this paper, we would like to point out that such synchronization analyses can also be applied to electroencephalogram (EEG) or magnetoencephalogram (MEG) data.

REFERENCES

[1] S. Ogawa, D. W. Tank, R. Menon, J.M. Ellerman, S.G. Kim, H. Merkle, K. Ugurbil, "Intrinsic signal changes accompanying sensory stimulation: Functional brain mapping with magnetic resonance imaging," Proceedings of the National Academy of Sciences, USA 1992, 89:5951–5955.

[2] J.D. Haynes, G. Rees, "Decoding mental states from brain activity in humans," Nature Reviews Neuroscience *200*, 7: pp. 523–534.

[3] R.L. Buckner, A.A. Snyder, A.L. Sanders, M.E. Raichle, J.C. Morris, "Functional brain imaging of young, nondemented, and demented older adult," Journal of Cognitive Neuroscience 2000, vol. 12:24–34.

[4] Y. He, L. Wang, Y. Zang, T. Tian, X. Zhang, K. Li, T. Jiang, "Regional coherence changes in the early stages of Alzheimer's disease: a combined structural and resting-state functional MRI study," Neuroimage 2007, vol. 35: 488–500.

[5] J. Li, Z.J. Wang, S.J. Palmer, M.J. McKeown, "Dynamic Bayesian network modeling of fMRI: A comparison of group-analysis methods," NeuroImage 2008, vol. 41; 398–407.

[6] V.D. Calhoun, T. Eichele, G. Pearlson, "Functional brain networks in Schizophrenia: a review," Frontiers in Neuroscience 2009, vol. 3:1–12.

[7] K.J. Friston, A.P. Holmes, K.J. Worsley, J.B. Poline, C.D. Frith, R.S.J. Frackowiak, "Statistical parametric maps in functional imaging: A general linear approach," Human Brain Mapping 1995, vol. 2:189–210.

[8] K.J. Friston, P. Rotshtein, J.J. Geng, P. Sterzer, R.N. Henson, "A critique of functional localisers," NeuroImage 2006, vol. 30:1077–1087.

[9] J. Talairach, P. Tournoux, "Co-Planar Stereotaxic Atlas of the Human Brain," Thieme, Stuttgart, Germany 1998.

[10] N. Tzourio-Mazoyer, B. Landeau, D. Papathanassiou, "Automated anatomical labeling of activations in SPM using a macroscopic anatomical parcellation of the MNI MRI single-subject brain," NeuroImage 2002, vol. 15: 273–289.

[11] B. Thirion, O. Faugeras, "Feature characterization in fMRI data: the information bottleneck approach," Medical Image Analysis 2004, vol. 8:403–419.

[12] D. Balslev, F.A. Nielsen, S.A. Frutiger, J.J. Sidtis, T.B. Christiansen, C. Svarer, S.C. Strother, D.A. Rottenberg, L.K. Hansen, O.B. Paulson, I. Law, "Cluster analysis of activity-time series in motor learning," Human Brain Mapping 2002, vol. 15:135–145.

[13] V.J. Schmithorst, S.K. Holland, "Comparison of three methods for generating group statistical inferences from independent component analysis of functional magnetic resonance imaging data," Journal of Magnetic Resonance Imaging, 2004, vol. 19:365–368.

[14] C. Baudelet, B. Gallez, "Cluster analysis of BOLD fMRI time series in tumors to study the heterogeneity of hemodynamic response to treatment," Magnetic Resonance in Medicine 2003, vol. 49:985–990.

[15] V.D. Calhoun, T. Adali, "Unmixing fMRI with independent component analysis," IEEE Engineering in Medicine and Biology Magazine, 2006, vol. 25:79–90.

[16] D. Liu, C. Yan, J. Ren, L. Yao, V.J. Kiviniemi, Y. Zang, "Using coherence to measure regional homogeneity of resting- state fMRI signal," Frontiers in System Neuroscience 2010, vol. 4:4-24.

[17] M.G. Kitzbichler, M.L. Smith, "Christensen SR, Bullmore E. Broadband criticality of human brain network synchronization," PLoS Computational Biology, 2009, vol. 5.

[18] SPM5, Statistical Parametric Mapping (SPM). Website: http://www.fil.ion.ucl.ac.uk/spm/ 2008.

[19] M.D. Fox, Z.Z. Snyder, J.M. Zacks, M.E. Raichle, "Coherent spontaneous activity accounts for trial-to-trial variability in human evoked brain responses," Nature Neuroscience 2006, vol. 9:23–25.

[20] K.J. Friston, A.P. Holmes, K.J. Worsley, "How many subjects constitute a study?," NeuroImage, 1999, vol. 10:1–5.

